Regular Solution Model for Asphaltene Precipitation from Bitumens and Solvents

Hussein Alboudwarej, Kamran Akbarzadeh, James Beck, William Y. Svrcek, and Harvey W. Yarranton
Dept. of Chemical and Petroleum Engineering, The University of Calgary, Calgary, Alberta, Canada, T2N 1N4

A regular solution theory liquid-liquid equilibrium model was developed to predict asphaltene precipitation from Western Canadian bitumens. The input parameters for the model are the mole fraction, molar volume, and solubility parameters for each component. Bitumens were divided into four main pseudo-components corresponding to SARA fractions: saturates, aromatics, resins, and asphaltenes. Asphaltenes were divided into fractions of different associated molar mass based on a Schultz-Zimm molar mass distribution. Asphaltene self-association was accounted for through the average molar mass of the distribution. The molar volumes and solubility parameters of the pseudo-components were calculated using solubility, density, and molar mass measurements. The model successfully predicted the effect of solvent type and associated molar mass on asphaltene precipitation for model oil and n-alkane systems. The model also predicted the onset and amount of asphaltene precipitation from bitumens.

Introduction

Asphaltenes are a solubility class of crude oils and are defined as the fraction that precipitates upon the addition of an *n*-alkane (usually *n*-pentane or *n*-heptane), but dissolves in aromatic solvents such as toluene. Asphaltenes can precipitate upon a change in pressure, temperature, and/or composition. For example, when pressure is drawn down around and within a wellbore, asphaltenes can precipitate and significantly reduce production. Also, when condensate diluent is added to heavy oils to reduce viscosity, asphaltene deposition can occur in surface facilities and pipelines. Treatment to remove or prevent the formation and deposition of solids increases operating costs. Therefore, it is desirable to prevent or mitigate asphaltene deposition. As a first step, it is necessary to predict the onset and amount of asphaltene precipitation.

Recent evidence suggests that asphaltenes are macromolecules that self-associate in a manner analogous to polymerization (Agrawala and Yarranton, 2001). Of the many approaches to modeling asphaltene precipitation (Andersen and Speight, 1999), regular solution theory is readily adapted to polymer-like systems and has been successfully applied to asphaltene-solvent systems (Yarranton and Masliyah, 1996). Regular solution theory incorporates the entropy and enthalpy of mixing of regular and athermal solutions. The model parameters are the mole fraction, molar volume, and solubility parameter for each component. The entropy of mixing of monodisperse polymer-like molecules can be accounted for using Flory (1941) and Huggins (1941) lattice theory. Hirschberg et al. (1984) used this approach to model asphaltene precipitation from crude oils, assuming a single component asphaltene fraction. Scott and Maget (1945a,b) adapted the model for polydisperse polymer solutions and the modified model was applied to asphaltene precipitation using a molar mass distribution for asphaltenes (Kawanaka et al., 1991). Funk and Prausnitz (1970) introduced an interaction parameter and this variation was also tested on asphaltene precipitation (Kawanaka et al., 1991; Andersen and Speight, 1999; Yang et al., 1999).

The major challenge in modeling asphaltene precipitation with regular solution theory is to characterize the asphaltenes in terms of the molar mass, molar volume, and solubility parameter distributions. Since asphaltenes are a mixture of tens of thousands of chemical species, asphaltene properties are not well defined. Also, when asphaltenes are lumped as a single component, it is difficult to accurately predict the amount of precipitation. An alternative approach is to divide the asphaltenes into fractions of different molar mass. The molar volume and solubility fraction of each asphaltene fraction are either calculated using an equation of state (EOS)

Correspondence concerning this article should be addressed to H. W. Yarranton.

(Hirschberg et al., 1984; Kawanaka et al., 1991; Cimino et al., 1995; Rassamdana et al., 1996) or estimated (Rassamdana et al., 1996; Anderson and Speight, 1999; Wang and Buckley, 2001). The EOS approach is attractive because it is predictive, but requires critical properties of the asphaltenes and other heavy crude oil fractions. These properties are not known and, in fact, are physically meaningless because heavy crude oil components decompose well below their critical point. On the other hand, estimated parameters have a limited range of applicability. Hence, there is a need to develop generally applicable correlations for asphaltene and other heavy component molar volumes and solubility parameters.

In this work, Hildebrand and Scott (1949, 1962) regular solution theory is used to model asphaltene precipitation from (a) mixtures of asphaltenes in toluene/n-alkane; (b) mixtures of bitumen/n-alkane at atmospheric conditions. The bitumen is separated into four main pseudo-components corresponding to SARA fractions (saturates, aromatics, resins, and asphaltenes). The saturates, aromatics, and resins are treated as single pseudocomponents. The asphaltenes are assumed to be a continuum of aggregates (self-associated asphaltenes) of increasing effective molar mass. The molar mass distribution is assumed to follow a Schultz-Zimm distribution function and the asphaltenes are divided into fractions of different "associated" molar mass based on this distribution. Molar volumes of the SARA fractions are calculated using density and molar mass measurements, while the solubility parameters for the SARA fractions are calculated using experimental solubility data. A liquid-liquid equilibrium was assumed with only the asphaltenes partitioning to the dense phase.

Experimental Methods

Chemicals and materials

Athabasca and Cold Lake bitumens, and Lloydminster heavy oil were obtained from Syncrude Canada Ltd., Imperial Oil Ltd., and Husky Oil Ltd., respectively. The Athabasca bitumen was an oilsand bitumen that had been processed to remove sand and water. The Cold Lake sample was recovered by a steam injection from an underground reservoir and had also been processed to remove sand and water. The Lloydminster heavy oil was a wellhead sample from a cyclic steam injection project and had not been processed. The Lloydminster sample contained water which was removed by diluting the heavy oil with n-heptane to a ratio of 0.8 cm^3 heptane/g bitumen. At this ratio, the density of the oil was reduced sufficiently for the water to settle. The supernatant was decanted and the n-heptane was removed in a rotary evaporator at 70°C under vacuum. Toluene, n-heptane, n-pentane, n-hexane, n-octane, and acetone were obtained from Aldrich Chemical Company and were 99%+ pure.

SARA Fractionation

Asphaltenes were precipitated from each bitumen or heavy oil with the addition of n-pentane for SARA fractionation or n-heptane for solubility experiments and property measurements. The final step of the n-heptane precipitation method involves washing an asphaltene filter cake. The extent of washing was varied to obtain, in order from least to most extensive washing: "Unwashed", "Filter-Washed", "Sonicator-Washed", and "Soxhlet-Washed" asphaltenes. The greater the extent of washing, the lower the resin content and the higher the molar mass. Details of the precipitation method are provided elsewhere (Alboudwarej et al., 2002).

Table 1. SARA Analysis (wt. %) of Bitumens and Heavy Oils

	Athabasca	Cold Lake	Lloydminster
Saturates	16.3	19.4	23.1
Aromatics	39.8	38.1	41.7
Resins	28.5	26.7	19.5
C_5-Asphaltenes and Solids*	15.4	15.8	15.7
C_5-Asphaltenes	14.6	15.3	15.1
Solids	0.8	0.5	0.6
Solids†	4.9	3.0	3.8

*Asphaltenes + solids extracted by n-pentane.
† Wt. % of total C_5-asphaltenes and solids.

Most asphaltene samples contain nonasphaltenic solids including sand, clay and adsorbed organics. Solids were removed by dissolving asphaltenes in toluene and centrifuging for 6 min at 3,500 rpm (900 Relative Centrifugal Force). The solids content for each bitumen was determined from the mass of solids in the asphaltene samples and the asphaltene yields. The bitumen solids content was determined and is given in Table 1. Saturates, aromatics and resins were extracted according to ASTM D2007M. The SARA analysis and solids content of the three bitumens and heavy oils are also reported in Table 1.

Molar mass measurements

Molar masses of SARA fractions were measured using vapor pressure osmometry as reported elsewhere (Yarranton et al., 2000; Agrawala and Yarranton, 2001; Akbarzadeh et al., 2001; Alboudwarej et al., 2002). All measurements were made in toluene at 50°C. Molar masses of saturates, aromatics, and resins are given in Table 2. Unlike the other SARA fractions, asphaltenes self-associate and the molar mass depends on both concentration and temperature (Yarranton et al., 2000). Therefore, the asphaltene molar masses were measured over a range of concentrations from 1 to 50 kg/m^3, as shown in Figure 1. The asphaltene monomer molar mass was estimated by extrapolating the low concentration molar mass trends to zero concentration. Estimated monomer molar masses for asphaltenes from each heavy oil and bitumen are given in Table 2. The average extrapolated asphaltene monomer molar mass was 1,800 g/mol. Average associated asphaltene molar masses are reported in the results and discussion. There is considerable scatter in VPO data particularly at low concentrations. The error in the reported molar

Table 2. Molar Masses (g/mol) of SARA Fractions in Toluene at 50°C

	Athabasca	Cold Lake	Lloydminster
Saturates	524	508	482
Aromatics	550	522	537
Resins	976	930	859
C_7-Asphaltenes (monomer)	2,200	1,400	1,800

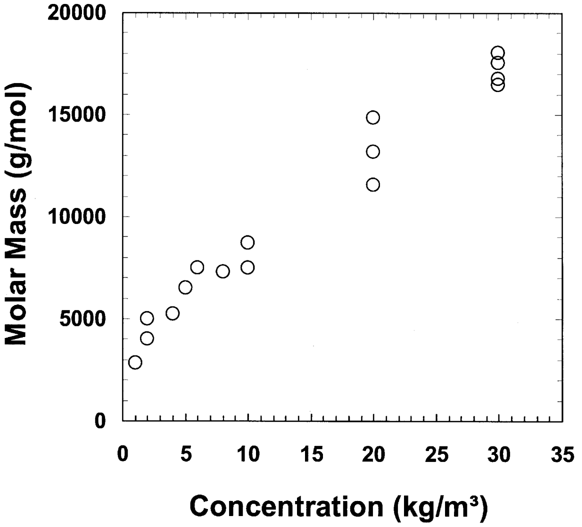

Figure 1. Effect of concentration on the average associated molar mass of Soxhlet-Washed Athabasca C_7-asphaltenes (adapted from Alboudwarej et al., 2002).

masses is approximately ±10% at asphaltene concentrations above 5 kg/m^3 and up to ±25% at lower concentrations.

Density measurements

Densities were measured with an Anton Paar DMA 46 density meter calibrated with demineralized water and air. The instrument precision is ± 0.0005 g/cm^3. Asphaltene densities were calculated indirectly from the densities of mixtures of asphaltenes in toluene as described elsewhere (Yarranton and Masliyah, 1996). Densities were accurate to ± 0.5 kg/m^3. Densities for saturates, aromatics, resins, and asphaltenes are given in Table 3.

Asphaltene precipitation and solubility measurements

Asphaltene precipitation and solubility measurements were performed gravimetrically in: (a) mixtures of 10 kg/m^3 of asphaltenes in toluene/*n*-alkane; (b) mixtures of bitumen/*n*-alkane. All measurements were taken at 23°C and atmospheric pressure. After preparing the mixtures, they were sonicated for 45 min and left to settle for 24 h. The mixtures were then centrifuged at 3,500 rpm (900 RCF) for 6 min. The supernatant was decanted and the asphaltenes were recovered, washed with the same solvent, and dried. For solutions of bitumen and solvents, asphaltene precipitation is reported as the weight fraction from the original bitumen. For solutions of asphaltenes and solvents, asphaltene precipitation is reported on a fractional basis; that is, the mass of precipitated asphaltenes divided by the total mass of asphaltenes. The reported precipitation curves are corrected to a solids-free basis. Note that the precipitation of solids-free asphaltenes and untreated asphaltenes was compared. The solids precipitated with the first asphaltenes to precipitate, but did not otherwise alter the onset or amount of asphaltene precipitation. The error in the solubility data is approximately ±5%.

Table 3. Measured Densities (kg/m^3) of Oils and Their SARA Fractions at 23°C

	Athabasca	Cold Lake	Lloydminster
Saturates	900	882	876
Aromatics	1,003	995	997
Resins	1,058	1,019	1,039
C_7-Asphaltenes	1,192	1,190	1,181

Regular Solution Model

It is still not certain if asphaltenes "precipitate" as a liquid phase or a solid phase. Multiple phase behavior, including V-L1-L2-S, has been observed for crude oils (Shelton and Yarborough, 1977; Shaw et al., 1997). Typically, multiple phases appear for mixtures that either contain very light hydrocarbons such as methane and ethane or for systems close to their bubble point. The existence or lack of multiple phases could not be confirmed experimentally for the systems under investigation. However, since the systems were well above the bubble point, it was assumed that there are only two phases. In this work, the dense phase is treated as a second liquid phase. Note that this form of the model is equivalent to that of an amorphous solid with a negligible heat of fusion.

For any two phases at equilibrium, the fugacities of each component in existing phases are equal and are given by

$$f_i = \gamma_i x_i f_i^0 \exp\left[\int_0^P \frac{v_i dP}{RT}\right] \tag{1}$$

from which the equilibrium ratio is defined as

$$K_i^{L_2L_1} = \frac{x_i^{L_2}}{x_i^{L_1}} = \left(\frac{\gamma_i^{L_1}}{\gamma_i^{L_2}}\right)\left(\frac{f_i^{0L_1}}{f_i^{0L_2}}\right)\exp\left[\int_0^P \frac{\Delta v_i dP}{RT}\right] \tag{2}$$

where K is the equilibrium ratio, i is the component, L_1 and L_2 are the light and dense phases, respectively, x is the mole fraction, γ is the activity coefficient, f^0 is the standard fugacity, v is the molar volume, P is pressure, R is the universal gas constant, and T is the absolute temperature.

For a liquid-liquid equilibrium, the terms $(f_i^{0L_1}/f_i^{0L_2})$ and $\exp\,[\int_0^P (\Delta v_i dp/RT)]$ are unity and Eq. 2 reduces to

$$K_i^{L_2L_1} = \frac{x_i^{L_2}}{x_i^{L_1}} = \left(\frac{\gamma_i^{L_1}}{\gamma_i^{L_2}}\right) \tag{3}$$

where the activity coefficient for a component in an athermal and regular solution is defined by Prausnitz et al. (1999) as

$$\ln \gamma_i^L = \ln \frac{v_i^L}{v_m^L} + 1 - \frac{v_i^L}{v_m^L} + \frac{v_i^L}{RT}\sum_j^n \sum_k^n \Phi_j \Phi_k \left(D_{ij} - 0.5 D_{jk}\right) \tag{4}$$

where subscript m stands for the mixture and Φ_i is the volume fraction defined as

$$\Phi_i = \frac{x_i v_i}{\sum x_i v_i} \tag{5}$$

and

$$D_{jk} = \left(\delta_j - \delta_k \right)^2 + 2 l_{jk} \delta_j \delta_k \tag{6}$$

where δ is the solubility parameter and l_{jk} is the interaction parameter between the two components j and k. For every component j, $l_{jj} = D_{jj} = 0$.

In this work, it was assumed that the interaction parameter between any of the components is zero; that is, $l_{jk} = 0$. In this case, Eq. 4 reduces to

$$\ln \gamma_i^L = \ln \frac{v_i^L}{v_m^L} + 1 - \frac{v_i^L}{v_m^L} + \frac{v_i^L}{RT}\left(\delta_i - \delta_m \right)^2 \tag{7}$$

where δ_m is the volume average of the solubility parameters of all the components in the mixture

$$\delta_m = \sum_i^m \Phi_i \delta_i \tag{8}$$

Experimental observations indicate that the dense phase material consists primarily of asphaltenes. Hence, to promote more rapid convergence, it is assumed that only asphaltenes partition to this phase. The asphaltenes are treated as a mixture of pseudo-components of different molar mass as well. Since the dense phase consists only of asphaltenes, it is assumed to be an ideal mixture of these asphaltene components. Therefore, the activity coefficients in the dense phase are unity and only the activity coefficients in the light phase are calculated. Equation 3 then reduces to

$$K_i = \gamma_i^{L_1} = \exp\left(\ln \frac{v_i^{L_1}}{v_m^{L_1}} + 1 - \frac{v_i^{L_1}}{v_m^{L_1}} + \frac{v_i^{L_1}}{RT}\left(\delta_i - \delta_m \right)^2 \right) \tag{9}$$

To test the ideal dense phase assumption, the model was run using both dense and light phase activity coefficients. The solubility predictions were similar to the case of an ideal dense phase. It appears that, when only asphaltenes are present in the dense phase, the entropic effects in the dense phase are small compared with those in the light phase.

The phase calculations are performed as follows (Rijkers and Heidemann, 1986):

(1) For a known solvent-to-bitumen ratio, the feed composition is calculated.

(2) The K values are initiated using the feed composition.

(3) The phase amounts are calculated using the Rachford-Rice method.

(4) The composition of the light liquid phase is updated and normalized.

(5) Convergence is checked.

(6) The K values are updated using the new composition.

(7) Return to Step No. 3 until convergence is achieved.

Note that there are many orders of magnitude difference between the equilibrium ratios of the asphaltenes and that of other components; therefore, some care was required to achieve convergence in the phase calculation program. For example, it was found that the bisection convergence method was more robust than the Newton-Raphson method when used to calculate the amount of each phase.

Fluid characterization

The required input data to the regular solution model are the mole fraction, molar volume, and solubility parameter for each (pseudo)component. In this work, the fluids are solutions of asphaltenes and mixed solvents or bitumen and n-alkanes. The solvent properties are known. The bitumens were divided into four fractions corresponding to the SARA fractions (saturates, aromatics, resins and asphaltenes). The saturates, aromatics, and resins were treated as individual pseudocomponents. Yarranton and Masliyah (1996) showed that to accurately predict the quantity of asphaltene precipitation, it is necessary to account for the distribution of molar volume and solubility parameter in the associated asphaltenes. Hence, the asphaltenes were divided into fractions of different associated molar mass. Details of the asphaltene discretization and the determination of molar volumes and solubility parameters for all the SARA fractions are discussed in detail below.

Asphaltene molar mass distribution

The asphaltenes were considered to be macromolecular aggregates of monodisperse asphaltene monomers. There is a distribution of aggregate sizes (molar mass) and, therefore, the asphaltenes were divided into fractions of different molar mass. A modified Schultz-Zimm distribution function (Akbarzadeh et al., 2002) was chosen to represent the asphaltene associated molar mass distribution because it was found to resemble molar mass distributions of asphaltenes measured with gel permeation chromatography and because it only requires a single fitting parameter r_{avg}. The modified Schultz-Zimm distribution is given by Eq. 10

$$f(r) = \frac{4(r-1)}{\left(r_{\text{avg}} - 1 \right)^2} \exp\left[-\frac{2(r-1)}{\left(r_{\text{avg}} - 1 \right)} \right] \tag{10}$$

where r is the aggregation parameter of each asphaltene molar mass fraction; that is, the molar mass of the aggregate divided by the monomer molar mass. r_{avg} is the average aggregation state of asphaltenes defined as the average molar mass of the distribution divided by the monomer molar mass.

The distribution was discretized into increments of constant Δr. The mass fraction of each segment was calculated from Eq. 11

$$x_i = \int_{r_i}^{r_{i+1}} f(r)\, dr \Big/ \int_{r_1}^{r_n} f(r)\, dr \tag{11}$$

and the average aggregation parameter for each fraction was calculated from Eq. 12

$$\bar{r}_i = \int_{r_i}^{r_{i+1}} r f(r)\, dr \Big/ \int_{r_i}^{r_{i+1}} f(r)\, dr \tag{12}$$

from which the average molar mass of each asphaltene fraction can be calculated as

$$M_i = \bar{r}_i M_{\text{monomer}} \tag{13}$$

In order to generate an asphaltene molar mass distribution, the following input data are required: the molar mass of the monomer; the average associated molar mass of the whole asphaltene sample; the upper limit of asphaltene molar mass distribution; and the number of asphaltene fractions. Monomer molar masses were determined with VPO. Given the high level of scatter in VPO measurements at low concentrations, and, for the sake of simplicity, an average asphaltene monomer molar mass of 1,800 g/mol was chosen for all oil samples. The average associated molar mass for each asphaltene sample was also measured with VPO. The asphaltene was divided into 30 fractions and a molar mass of 30,000 g/mol was employed for the heaviest asphaltene fraction. The modeling results were not sensitive to increases in the molar mass of the heaviest fraction beyond 30,000 g/mol or to the number of asphaltene fractions beyond 30.

Asphaltene molar volume

Molar volume is the ratio of molar mass to density. Yarranton and Masliyah (1996) demonstrated that it is necessary to account for both the molar mass and density distribution of the asphaltenes to obtain accurate predictions of asphaltene precipitation using a regular solution model. A constant density was not sufficient. Therefore, to find the molar volume for each asphaltene fraction, it was necessary to relate density to molar mass. Densities and associated molar masses were previously measured for asphaltenes from different sources and for different extraction methods (Yarranton and Masliyah, 1996; Yarranton et al., 2000; Akbarzadeh et al., 2001; Alboudwarej et al., 2002). The molar masses were measured with VPO at 50°C in toluene, but the density measurements were made at 23°C. Asphaltene associated molar mass is sensitive to temperature (Yarranton et al., 2000) and, since measurements could not be obtained at 23°C, the molar mass measurements were extrapolated to 23°C. Molar masses measured at 75°C and 50°C (Yarranton et al., 2000) were linearly extrapolated to 23°C. The extrapolated molar masses at 23°C were approximately 20% higher than those at 50°C. Hence, a 20% correction was applied to all of the molar mass data. The corresponding densities and molar masses are shown as open symbols in Figure 2.

In addition, unwashed and soxhlet-Washed Athabasca asphaltene samples were separated into two high and two low molar mass fractions. The whole asphaltene was dissolved in toluene and then approximately 50 wt. % of the asphaltene was precipitated by adding an appropriate volume of n-heptane. The molar mass of each fraction was measured with VPO in toluene at 50°C and an asphaltene concentration of 40 kg/m^3. Densities were measured for the same fractions at both 50°C and 70°C. The densities were insensitive to temperature within the scatter of the data. The corresponding densities and molar masses are plotted as solid symbols in Figure 2. Since aromatics, resins, and asphaltenes are all polynuclear aromatics, the data presented in Figure 2 also included aromatics and resins.

A correlation of density to molar mass cannot be obtained directly from Figure 2 because the data points are average quantities for a polydisperse mixture. Instead, the average density for each asphaltene fraction is computed as follows

$$\rho_i = \int_{r_i}^{r_{i+1}} \rho(r) f(r) dr \Bigg/ \int_{r_i}^{r_{i+1}} f(r) dr \qquad (14)$$

Linear, power law and logarithmic density distribution functions were used to calculate average asphaltene densities and compared with measured densities that included and excluded the aromatics and resins. Each density distribution function was tested with the solubility model on the full set of available precipitation data. The "best" results were obtained when the density power law function included the resin and aromatic data (Eq. 15)

$$\rho = 670\, M^{0.0639} \qquad (15)$$

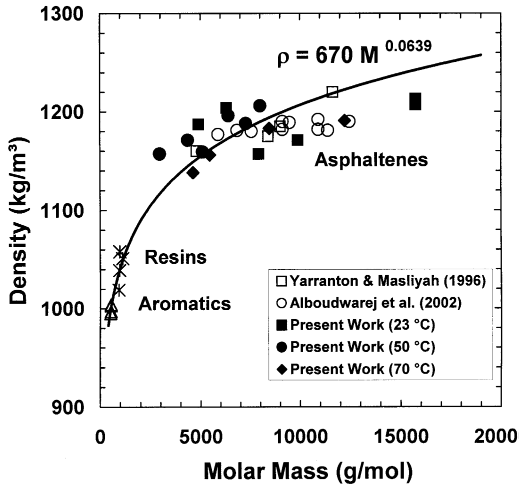

Figure 2. Density of Athabasca asphaltenes, resins, and aromatics.

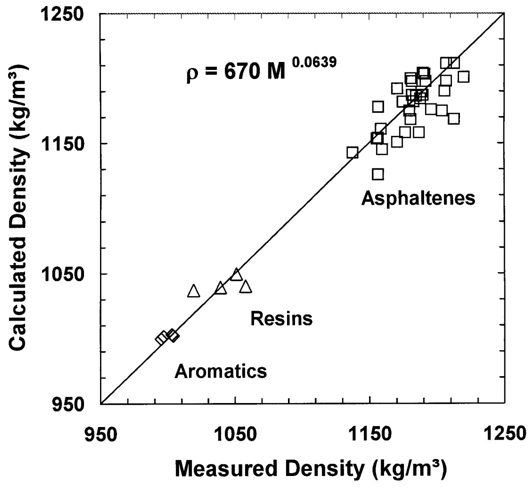

Figure 3. Comparison of measured and calculated Athabasca asphaltenes, resins, and aromatics densities.

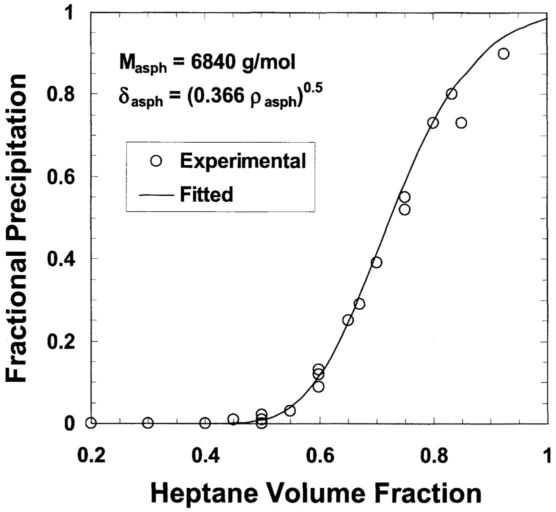

Figure 4. Fractional precipitation of Unwashed Athabasca asphaltenes from solutions of *n*-heptane and toluene.

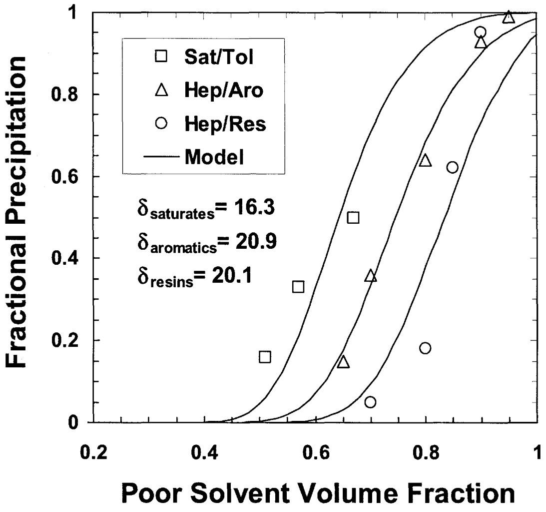

Figure 5. Fractional precipitation of Unwashed Athabasca asphaltenes from solutions of saturates and toluene, aromatics and heptane, or resins and heptane.

where ρ is the asphaltene density in kg/m^3 and M is the molar mass in g/mol. Figure 3 presents a comparison of measured densities to calculated densities using Eq. 15. The average absolute relative deviation is 1.07%.

One potential inconsistency that arises is: if asphaltenes are aggregates of monodisperse monomers, why does the asphaltene density change with molar mass? A possible explanation is that the monomers are in fact polydisperse and the denser monomers are concentrated in the larger aggregates. Another possibility is that the monomer density changes when it becomes part of an aggregate.

Asphaltene solubility parameter

Yarranton and Masliyah (1996) recommended the following semi-empirical correlation to determine the solubility parameter of asphaltenes

$$\delta = (A\rho)^{1/2} \tag{16}$$

where δ is the solubility parameter (MPa$^{0.5}$), and A is the monomer heat of vaporization (kJ/g). The constant A is determined by fitting the model to one set of asphaltene-n-heptane-toluene precipitation data. In this case, a value of 0.366 kJ/g was determined for A from the solubility of Athabasca Unwashed C_7-asphaltenes in a mixture of n-heptane and toluene (Figure 4). Note, the r_{avg} used for the model fit was determined from the measured molar mass of Unwashed Athabasca C_7-asphaltenes (5,700 g/mol) corrected by +20%. The value A was then fixed for all other model predictions.

Saturates, aromatics, resins and solvents properties

Molar volumes for the solvents were calculated using the Hankinson-Brobst-Thomson (HBT) method (Reid et al., 1989). Solubility parameters for the solvents were calculated as follows

$$\delta = \left(\frac{\Delta H^{\text{vap}} - RT}{v} \right)^{1/2} \tag{17}$$

where ΔH^{vap} is the heat of vaporization reported in the literature (Perry and Green, 1997). The molar volumes of saturates, aromatics, and resins were determined from the molar masses and densities presented in Tables 2 and 3. The solubility parameters of the saturate and aromatics were determined by fitting the solubility model to asphaltene-saturate-toluene and asphaltene-n-heptane-aromatics solubility data, respectively. The corresponding measured and fitted fractional asphaltene precipitation curves are shown in Figure 5. The solubility parameters of saturates and aromatics were found to be 16.3 and 20.9 MPa$^{0.5}$, respectively.

Since the aggregation state of asphaltenes changes in the presence of resins (Agrawala and Yarranton, 2001), asphaltene-n-heptane-resin solubility data could not be used to back-calculate the solubility parameter of resins. Since resins resemble asphaltene monomers, it was assumed that the solubility parameter of resins is equal to that of monomer asphaltenes, 20.1 MPa$^{0.5}$. Figure 5 shows the measured and predicted solubility of asphaltenes in solutions of n-heptane and resins. Although the change in asphaltene molar mass with resin addition is not included, the predicted fractional precipitation matches the magnitude and trend of the data quite well.

Results and Discussion

Asphaltene + toluene/n-alkane systems

Figure 6 shows the measured and predicted fractional precipitation of Unwashed Athabasca asphaltenes in solutions of toluene and a series of n-alkanes. In general, the predicted fractional precipitation decreases in the order of $C_5 > C_6 >$

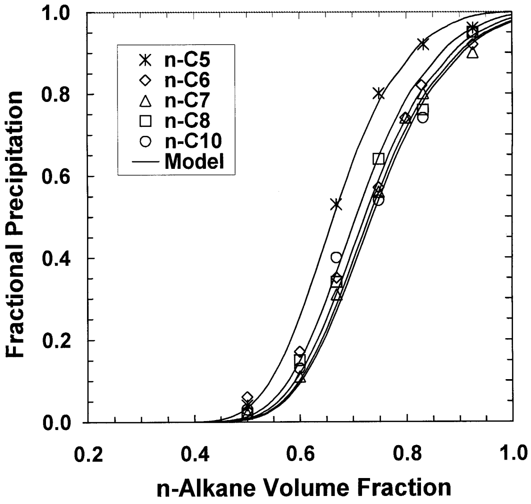

Figure 6. Effect of *n*-alkane carbon number on the fractional precipitation of Unwashed Athabasca asphaltenes from *n*-alkane/toluene solutions.

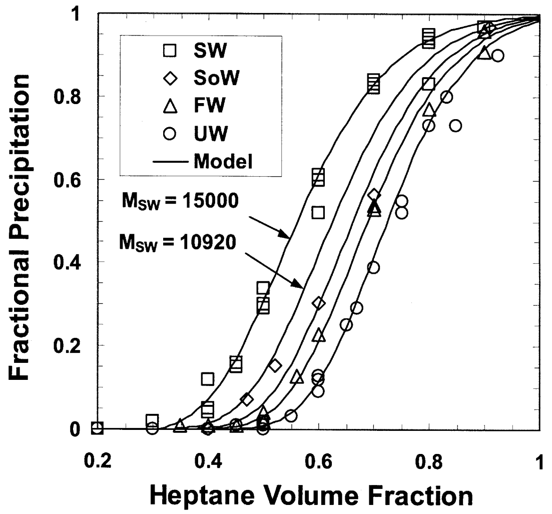

Figure 7. Effect of asphaltene associated molar mass on the fractional precipitation of Unwashed Athabasca asphaltenes from solutions of *n*-heptane and toluene.

$C_7 > C_8 > C_{10}$ as expected from previous observations (Speight, 1999). However, the trend is partially obscured due to the scatter in the solubility data and the small difference in the solubility curves in the higher carbon number alkanes. Recall that the model was fitted to asphaltene precipitation from solutions of toluene and *n*-heptane. With no adjustment of input parameters or use of interaction parameters, the model predicts the remaining precipitation curves in *n*-alkanes with an average absolute relative deviation (AARD) of 6.7% (1.7% for *n*-pentane and 12.7% for *n*-octane). These good predictions confirm Mannistu et al.'s (1997) results where a similar regular solution model was employed to predict the effect of *n*-alkanes on asphaltene precipitation.

Figure 7 shows the effect of asphaltene associated molar mass on asphaltene precipitation from solutions of toluene and *n*-heptane. The asphaltenes are Unwashed (UW), Filter-Washed (FW), Sonicator-Washed (SoW), and Soxhlet-Washed (SW) Athabasca C_7-asphaltenes. The molar masses were measured in toluene at an asphaltene concentration of 10 kg/m^3 and the temperature corrected values are given in Table 4. The molar masses used to fit the precipitation data are also given in Table 4. The corrected molar masses for Unwashed and Sonicator-Washed asphaltenes were used directly to fit the data with an AARD of 6.4% and 12.9%, respectively. The corrected molar mass of Filter-Washed asphaltenes, 9,500 g/mol was not on trend and was, therefore, not used in the model. Instead, a molar mass of 8,000 g/mol was used and resulted in an AARD of 4.5%. For Soxhlet-Washed asphaltenes the corrected molar mass is 10,920 g/mol. When this value is used, the AARD is 31.7%. However, a molar mass of 15,000 g/mol fits the data quite well with an AARD of 5.0%. Given the scatter in VPO measurements of asphaltene molar masses, it is probable that the measured molar mass for the Soxhlet asphaltenes is too low. It remains a challenge to obtain accurate solubility predictions based on measured molar masses of limited accuracy. However, it is clear that the extent of asphaltene association strongly influences asphaltene solubility and must be accounted for.

Bitumen + n-alkane systems

The asphaltene fractional yield data for the Lloydminster heavy oil diluted with various *n*-alkanes are presented in Figure 8. As for the asphaltene-solvent systems, asphaltene solubility decreases as the *n*-alkane carbon number decreases. Unlike the asphaltene solvent systems, the associated molar mass of the asphaltenes in bitumen is unknown. Therefore, the average associated molar mass of the asphaltenes must be estimated. The model was "fit" to the Lloydminster-*n*-heptane system using an average asphaltene molar mass of 3,275 g/mol resulting in an AARD of 3.5%. It was also assumed that the average molar mass did not change upon the addition of *n*-alkanes. The model was then used to successfully predict the onset of precipitation and asphaltene fractional yields for bitumen and *n*-pentane, *n*-hexane, and *n*-octane solutions. The resulting average AARD for the Lloydminster-*n*-alkane systems is 13.4%.

Asphaltene precipitation from Athabasca and Cold Lake bitumens with *n*-alkanes are shown in Figures 9 and 10, respectively. The model was fit using only the *n*-heptane data and an average asphaltene molar mass of 3,075 g/mol for Athabasca bitumen and 2,925 g/mol for Cold Lake bitumen. The model was again used to predict asphaltene precipitation

Table 4. Molar Masses (g/mol) of Different Degree Washed Athabasca Asphaltenes

	Measured	Fitted	Fitted*
Unwashed	5,700	5,700	6,840
Filter-Washed	7,900	6,700	8,040
Sonicator-Washed	7,600	7,600	9,120
Soxhlet-Washed	9,100	12,500	15,000

*Increased by 20% for temperature correction @ 23 °C.

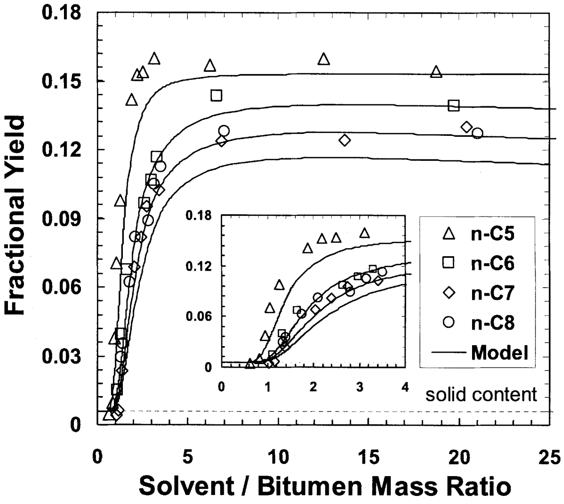

Figure 8. Fractional asphaltene yield from Lloydminster bitumen diluted with *n*-pentane, *n*-hexane, *n*-heptane or *n*-octane.

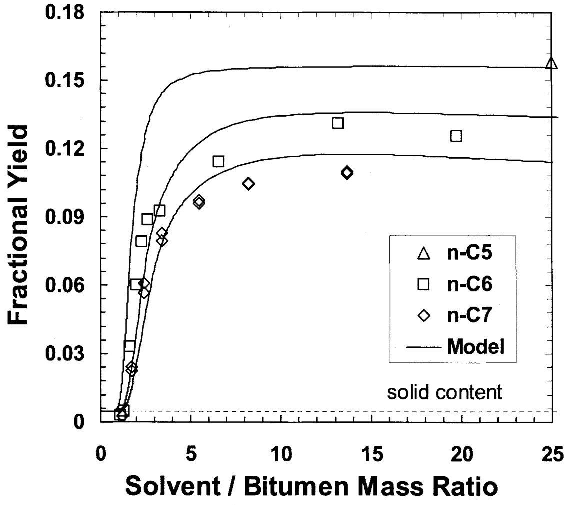

Figure 10. Fractional asphaltene yield from Cold Lake bitumen diluted with *n*-pentane, *n*-hexane, or *n*-heptane.

for other *n*-alkane solvents. The overall AARD for Athabasca bitumen-*n*-alkane systems is 6% and for Cold Lake bitumen-*n*-alkane systems is 11.8%.

The average associated molar masses used to fit the precipitation data are 3,275, 3,075 and 2,925 g/mol for Lloydminster heavy oil, Athabasca bitumen and Cold Lake bitumen, respectively. The variation in the average molar masses is small, but it is interesting to note that the highest molar mass used was for the Lloydminster heavy oil, which has the lowest resin-to-asphaltene ratio (Table 1). Asphaltene association is known to decrease as the resin-to-asphaltene ratio increases; hence, the average asphaltene molar mass is expected to be low in bitumens in general and lowest for bitumens with the highest resin-to-asphaltene ratio.

In all cases, the tuned model predicted both the onset and the ultimate amount of precipitation with reasonable accuracy (AARD < 15%). The model underpredicted the amount of precipitation at intermediate solvent-to-bitumen ratios. A possible explanation is that the molar mass distribution of the asphaltenes in bitumen does not follow the Schultz-Zimm distribution. Changing the distribution will change the shape of the predicted yield curve. Another possible explanation is that the average molar mass of the asphaltenes increases when a *n*-alkane is added to the bitumen. If the molar mass is greater than predicted, the model will underestimate the amount of precipitation at intermediate yields. The high yield prediction is less sensitive, because most of the asphaltenes precipitate at this point whatever the average molar mass.

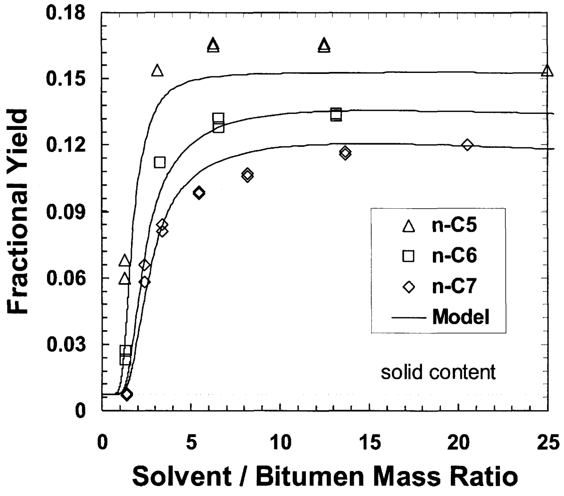

Figure 9. Fractional asphaltene yield from Athabasca bitumen diluted with *n*-pentane, *n*-hexane or *n*-heptane.

Conclusions

A regular solution model successfully fitted and predicted asphaltene precipitation in solvent mixtures. Asphaltenes were treated as a mixture of fractions of different molar mass, molar volume, and solubility parameter. Asphaltene self-association was accounted for through an input molar mass distribution that followed a Schultz-Zimm distribution function generated from the average associated molar mass. Molar volumes of the asphaltene fractions were determined from measured molar masses and densities. The model was tuned to one set of asphaltene and solvent data to find the solubility parameter of asphaltenes. The model predicted the onset and amount of precipitation with an AARD less than 13% for asphaltenes in solutions of toluene and *n*-alkanes and for asphaltenes of different molar mass in solutions of *n*-heptane and toluene.

Two bitumens and a heavy oil were characterized in terms of SARA fractions. The molar volume and solubility parameter of the fractions were determined from molar mass, density, and asphaltene precipitation measurements. Since the average associated molar mass of asphaltenes in bitumen is unknown, it was estimated by fitting the model to precipitation data from solutions of bitumen and *n*-heptane. Predictions were made for solutions of bitumen and *n*-pentane and *n*-hexane. The fitted and predicted onset and amount of precipitation was in good agreement with the experimental data in all cases.

Acknowledgments

The authors would like to thank Professor R. A. Heidemann for his valuable discussions on asphaltene phase calculations and Mr. Paul Chernik and Ms. Danuta Sztukowski for performing some of the experiments. Financial support from the Natural Sciences and Engineering Research Council of Canada (NSERC) is appreciated. We also thank Syncrude Canada Ltd., Imperial Oil Ltd. and Husky Oil Ltd. for supplying oil samples.

Literature Cited

Agrawala, M., and H. W. Yarranton, "Asphaltene Association Model Analogous to Linear Polymerization," *Ind. and Eng. Chemistry Res.*, **40**, 4664 (2001).

Akbarzadeh, K., Sh. Ayatollahi, M. Moshfeghian, H. Alboudwarej, and H. W. Yarranton, "Estimation of the SARA Fraction Properties Using the SRK EOS," CIPC Paper No. 2001-122, Canadian Int. Petroleum Conf., Calgary, Canada (June 12–14, 2001).

Akbarzadeh, K., Sh. Ayatollahi, M. Moshfeghian, H. Alboudwarej, W. Y. Svrcek, and H. W. Yarranton, "Prediction of Asphaltene Precipitation with a Modified SRK EOS, Proc. of 3rd Int. Conf. on Petroleum Phase Behavior and Fouling", AIChE Meeting, New Orleans, LA, 218 (Mar. 9-14, 2002).

Alboudwarej, H., J. Beck, W. Y. Svrcek, H. W. Yarranton, and K. Akbarzedeh, "Sensitivity of Asphaltene Properties to Extraction Techniques," *Energy & Fuels*, **16**, 462 (2002).

Andersen, S. I., and J. G. Speight, "Thermodynamic Models for Asphaltene Solubility and Precipitation," *J. of Petroleum Sci. and Eng.,* **22**, 53 (1999).

Cimino, R., S. Correra, and P. A. Sacomani, "Thermodynamic Models for Prediction of Asphaltene Deposition,"SPE paper No. 28993, Int. Symp. on Oilfield Chemistry, San Antonio, TX (Feb. 14–17, 1995).

Flory, P. J., "Thermodynamics of High Polymer Solutions," *J. of Chem. Physics*, **9**, 660 (1941).

Funk, E. W., and J. M. Prausnitz, "First Born Approximation Cross Sections for Electron Loss from Fast Hydrogen Atoms Passing Through Atomic Helium and Fast Helium Atoms Passing Through Atomic Hydrogen and Helium," *Ind. and Eng. Chemistry*, **62**, 8 (1970).

Hildebrand, J., and R. Scott, *Solubility of Non-Electrolytes*, 3rd ed., Reinhold, New York (1949).

Hildebrand, J., and R. Scott, *Regular Solutions*, Prentice Hall, Englewood Cliffs, NJ (1962).

Hirschberg, A., L. N. J. DeJong, B. A. Schipper, and J. G. Meijer, "Influence of Temperature and Pressure on Asphaltene Flocculation," *SPE J.*, 283 (June 1984).

Huggins, M. L., "Solutions of Long Chain Compounds," *J. of Chem. Physics*, **9**, 440 (1941).

Kawanaka, S., S. J. Park, and G. A. Mansoori, "Organic Deposition from Reservoir Fluids: a Thermodynamic Predictive Technique," *SPE Reservoir Eng.*, 185 (May 1991).

Mannistu, K. D., H. W. Yarranton, and J. H. Masliyah, "Solubility Modeling of Asphaltenes in Organic Solvents," *Energy & Fuels*, **11**, 615 (1997).

Perry, R. H., and D. Green, *Perry's Chemical Engineers' Handbook*, 7th ed., McGraw-Hill, New York (1997).

Prausnitz, J. M., R. N. Lichtenthaler, and E. G. D. Azevedo, *Molecular Thermodynamics of Fluid Phase Equilibria*, 3rd ed. Prentice Hall PTR, Upper Saddle River, NJ (1999).

Rassamdana, H., B. Dabir, M. Nematy, M. Farhani, and M. Sahimi, "Asphalt Flocculation and Deposition: I. The Onset of Precipitation," *AIChE J.*, **42**, 10 (1996).

Reid, R. C., J. M. Prausnitz, and B. E. Poling, *The Properties of Gases & Liquids*, 4th ed., McGraw-Hill, New York (1989).

Rijkers, M. P. W., and R. A. Heidemann, *Convergence Behavior of Single-Stage Flash Calculations, Article in Equations of State, Theories and Applications,* K. C. Chao and R. L. Robinson, Jr., eds., ACS Symposium Series 300, Washington, DC (1986).

Scott, R. L., and M. Magat, "The Thermodynamics of High-Polymer Solutions: I. The Free Energy of Mixing of Solvents and Polymers of Heterogeneous Distribution," *J. of Chem. Physics*, **13**, 172 (1945a).

Scott, R. L., and M. Magat, "The Thermodynamics of High-Polymer Solutions: II. The Solubility and Fractionation of a Polymer of Heterogeneous Distribution," *J. of Chem. Physics*, **13**, 178 (1945b).

Shaw, J. M., T. W. deLoos, and J. de Swaan Arons, "An Explanation for Solid-Liquid-Liquid-Vapor Phase Behavior in Reservoir Fluids," *Petroleum Sci. and Technol.*, **15**, 503 (1997).

Shelton, J. L., and L. Yarborough, "Multiple Phase Behavior in Porous Media during CO_2 or Rich-Gas Flooding," *J. of Petroleum Technol.*, *(SPE No. 5827)*, 1171 (Sept. 1977).

Speight, J. G., *The Chemistry and Technology of Petroleum*, Third ed., Marcel Decker, New York (1999).

Wang, J. X., and J. S. Buckley, "A Two-Component Solubility Model of the Onset of Asphaltene Flocculation in Crude Oils," *Energy & Fuels*, **15**, 1004 (2001).

Yang, Z., G. F. Ma, X. S. Lin, J. T. Yang, and T. M. Guo, "Experimental and Modeling Studies on the Asphaltene Precipitation in Degassed and Gas-injected Reservoir Oils," *Fluid Phase Equilibria*, **157**, 143 (1999).

Yarranton, H. W., and J. H. Masliyah, "Molar Mass Distribution and Solubility Modeling of Asphaltenes," *AIChE J.*, **42**, 3533 (1996).

Yarranton, H. W., H. Alboudwarej, and R. Jakher, "Investigation of Asphaltene Association with Vapor Pressure Osmometry and Interfacial Tension Measurements," *Ind. and Eng. Chemistry Res.*, **39**, 2916 (2000).

Manuscript received Nov. 27, 2002, revision received Apr. 8, 2003, and final revision received Jul. 18, 2003.